IEEE Access
Multidisciplinary | Rapid Review | Open Access Journal

Received February 19, 2020, accepted March 9, 2020, date of publication March 13, 2020, date of current version March 23, 2020.

Digital Object Identifier 10.1109/ACCESS.2020.2980736

Design and Evaluation of a Reliable Low-Cost Atmospheric Pollution Station in Urban Environment

GALO D. ASTUDILLO[1], LUIS E. GARZA-CASTAÑON[1], AND LUIS I. MINCHALA AVILA[2], (Senior Member, IEEE)

[1]School of Engineering and Sciences, Tecnológico de Monterrey, Monterrey 64849, Mexico
[2]School of Engineering and Sciences, Tecnológico de Monterrey–Guadalajara, Guadalajara 45201, Mexico

Corresponding author: Luis E. Garza-Castañon (legarza@tec.mx)

This work was supported in part by CONACyT, Mexico, and in part by Aixware Technologies, Monterrey NL, México.

ABSTRACT The pollution of the air constitutes an environmental risk to health, crops, animals, forests and water. There are several policies for reducing air pollution regarding industry, energy, transportation, and agriculture. Unfortunately, there is limited monitoring of the air quality in cities and rural areas for supervising the accomplishment of these policies. Reliable monitoring of air pollutants is, typically, based on expensive fixed stations, which constitutes a barrier to tackle. This research presents the design, implementation and evaluation of a small, low-cost, station for monitoring atmospheric pollution. The prototype registers ozone (O_3) and carbon monoxide (CO) using inexpensive sensors. To assure high reliability of the measurements obtained by the sensors installed in this station, it is proposed a calibration procedure based on the selection of the best performance analysis of the following machine learning techniques: multiple linear regression, artificial neural networks, and random forest. Additionally, a decision rule is implemented to select an optimal combination of sensors for the estimation models, while the sample timestamp is considered as a temporal heuristic at the input of the system, assuming similarities in the daily environmental dynamics. In order to test the station in a realistic scenario, the calibration and evaluation sets were taken in two different time frames of one and two months, respectively. The overall process was implemented with reference data coming from a certified air quality fixed station in the city of Cuenca - Ecuador. Experimental results showed that the real-time reports of ozone provided by the prototype are quite similar to the fixed station during the evaluation period, with a resulting correlation of up to $r = 0.92$ and $r = 0.91$ in the calibration and evaluation set, respectively. However, signal drift and aging in CO_x sensors diminished the accuracy of carbon monoxide calibration models, resulting in lower correlation ($r \leq 0.76$) with the evaluation set.

INDEX TERMS Low-cost sensors, neural networks, random forest, pollution, air monitoring, calibration.

I. INTRODUCTION

Air pollution represents a serious risk to health when, consciously or unconsciously, persons expose themselves for prolonged periods of time while the contaminant levels are high. According to the World Health Organization (WHO), there are approximately 4.2 million deaths due to exposure to air pollution (outdoors), 3.8 million deaths from dirty cook stoves and fuels per year, and 91% of total population live in areas that exceed the maximum concentrations allowed by the WHO [1]–[3]. Moreover, research shows the effect of several pollutants in human health, such as reduction of intelligence in kids [4], deterioration of cardiopulmonary health conditions [5], lung cancer [6], low birth weight of children [7]. Although the growth of emissions of some polluting gases has declined in the last two decades, the annual number of deaths from this cause keeps growing [8]. The impact is not limited to the environment and human health; more precisely, it has a high economic burden (estimated to be 3.0 trillion USD in 2010) [9]. In fact, it has become the second most important concern in Europe, after climate change [10]. In consequence, deploying stations to monitor and trace regulated pollutants has become of real importance for governmental entities as well as citizens, and several directives establish the

The associate editor coordinating the review of this manuscript and approving it for publication was Quinn Qiao.

maximum recommended pollutant concentrations together with the standards that the air monitoring equipment must meet [11], [12].

Traditional fixed air quality monitoring (FAM) stations have several limitations that include high costs of installation, operation and maintenance, ample mounting space ($\sim 8\ m^2$), and are inaccessible to the public. These conditions restraint the deployment of real-time monitoring networks in urban/rural places, especially in countries with a marginal public budget to afford at least one of these terminals. Besides, it is difficult to install such stations in neighborhoods / sectors of a metropolis to obtain spatial and temporal information on the concentration of polluting gases. To meet the requirements of an adequate measurement of air pollutants, low-cost (<300 USD), portable/small, low-weight monitoring stations are being developed [13]–[20] and Real-Time Affordable Multi-Pollutant (RAMP) monitors are aimed to fulfill the needs of these new systems [21]–[23].

An ideal RAMP monitor is expected to produce stable measurements with strong sensitiveness and high selectiveness towards the pollutants of interest. However, low-cost sensors performance differs from controlled conditions (*i.e.* laboratory) to stochastic environments (*i.e.* urban/rural areas), as variations occur spatially and temporally [24]. In addition, as described in [25], the measurement error could also be caused by the sensor internal limitations: non-linear response, signal drift, dynamic boundaries, systematic errors. Therefore, actual research efforts are focused on calibration techniques to mitigate these undesired effects, increasing the reliability and robustness of low-cost sensors to comply with data quality criteria in applications requiring accuracy for regulation purposes or scientific monitoring. In consequence, air composition sensed by RAMP monitors can't rely solely on filtered data from low-cost sensors. Additional environmental information needs to be included in the estimation model. As result, calibrating methods are required to improve accuracy, reduce estimation error and unwanted environmental side effects on sensors, and adjust cross-sensitivity so as to improve overall estimation. Machine learning techniques such as Multilayer Perceptron (MLP) in Artificial Neural Networks (ANN), can produce better approximations than multiple linear regression (MLR) [26], [27]; however, for some pollutants, hybrid methods combining linear and non-linear techniques can produce more accurate results [28], [29]. In addition to hybrid methods, other variants in machine learning showed to ameliorate the classic ANN, by including correction factors (temperature (T), relative humidity (RH)) or temporal information (previous samples) of the environment with Dynamic Neural Networks (DNN) [30], [31], utilizing Random Forest (RF) [32], [33], k-Nearest Neighbors (k-NN) [33], Support Vector Regression (SVR) [33], [34], or adding Fuzzy Logic for qualitative calibration [35] and prediction [36].

There are mainly two ways to evaluate the performance of the RAMP stations. For instance, in a three months experiment, the evaluation procedure may use randomly selected sub-samples from the whole sampling space, which may include data generated at the beginning as well as at the end of the experiment, resulting in a trained model with statistical assessment that may not include how the performance of the system is affected over time. A more realistic evaluation of the system would be for instance, to perform the calibration within the first month of operation, and measuring the accuracy during the next two months. This perspective is of importance because the quality of the information (QoI) generated by the RAMP monitor diminishes with time.

This research proposes the use of low-cost, portable stations that offer reliable measurements thanks to calibration procedures which use estimation models with inputs coming from different sensors combinations and machine learning algorithms. In addition, we evaluate our methodology in a different time frame in which the models were trained, in order to obtain a more realistic perspective of the operational limitations.

Among the most important pollutants in the atmosphere are: ozone (O_3), carbon monoxide (CO), nitrogen oxides (NO_x), sulfur dioxide (SO_2) and particulate matter (PM_{10}, $PM_{2.5}$) [3]. However, the proposal described in this article estimates only the concentration of ozone (in parts per billion (ppb)) and carbon monoxide (in parts per million (ppm)). At a later stage of the project, it is intended to incorporate more sensors.

The main contributions of this article are:

- A general procedure to build and calibrate a RAMP monitor.
- A decision rule to select an optimal sensor combination based on a performance index that considers the correlation and error from an estimation model and the reference values.
- A heuristic rule to be included in the estimation model to increase the correlation and reduce estimation error, specially in urban deployment with similar environmental dynamics.
- Quantitative analysis of three calibration methods by using a customized performance index which combines spatiotemporal information from the evaluation data obtained from a certified FAM.

This paper is organized as follows: Section II summarizes previous research in calibration techniques for air composition measurement with low-cost gas sensors. Also, several systems and state-of-the-art methodologies are described. Section III shows the physical realization and location of the RAMP monitor. In addition, it presents the official FAM station that will be used as reference. Section IV describes the validation methodology and mathematical tools. Section V presents the calibration procedure: sensors combination analysis and machine learning-based methodology. Section VI presents the overall results of this research, separating the calibrations and evaluation sets for ozone and carbon monoxide. Finally, conclusions are drawn in Section VII, discussing several considerations and future work.

TABLE 1. Calibration methods for several target pollutants, including O_3 or CO_x.

Target Pollutant(s)	System	Calibration Technique	Variable Combination
O_3, NO_2	Spinelle et al, 2015 [26]	LR, MLR, ANN	$O_3 + CO, O_3, NO_2$
O_3, NO_x	Esposito et al, 2016 [30]	MLR, ANN, NARX	$O_3 + NO, NO_2, T, RH$
O_3, CO, NO_2, SO_2	Jiao et al, 2016 [37]	LR, MLR	$O_3 + T, RH, A$ $CO + T, A$
O_3	Pang et al, 2017 [38]	LR	$O_3 + RH$
CO_2	Martin et al, 2017 [39]	MLR	$CO_2 + P, T, Q$
O_3, NO_x	*Barakeh et al, 2017 [36]	ANN	$O_3 + TS, T, RH$
CO_x, NO	Spinelle et al, 2017 [27]	LR, MLR, ANN	$CO + NO_2, CO_2, T, RH$
O_3, CO_x, NO_2	Zimmerman et al, 2018 [32]	MLR, RF	$CO + NO_2, O_3, CO_2, T, RH$ $O_3 + NO_2, CO, CO_2, T, RH$
O_3, CO_x, NO_x, SO_2	Pang et al, 2018 [40]	MLR	$O_3 + NO_2, NO, CO_2, RH$ $CO + O_3, NO_2, CO_2, RH$
O_3, CO	Topalović et al, 2019 [41]	LR, MLR, ANN	$O_3 + A, NO$ $CO + PM_{2.5}, NO_2$
O_3	Ferrer-Cid et al. 2019 [33]	MLR, k-NN, RF, SVR	$O_3 + NO_2, T, RH$

* Model for qualitative interpretation of pollutant concentrations.
Note 1: T - temperature, RH – relative humidity, P – pressure, Q – vapor water, A – aging, TS – time stamp.
Note 2: LR – linear regression, MLR – multivariate linear regression, ANN – artificial neural network, k-NN - k-nearest neighbors ,RF – random forest, NARX – nonlinear autoregressive with exogenous inputs network.

II. LITERATURE REVIEW

A. BACKGROUND

The global effects of air pollution have led to the implementation of control policies with the installation of certified air monitoring stations that would allow the enforcement of such protocols. However, a large scale deployment of fixed air monitoring stations is not feasible due to economic and/or operational limitations. Subsequently, affordable, automated and portable stations may provide an alternative solution. Nonetheless, the typical sensors embedded in the RAMP monitors (usually electro-chemical or metal-oxide transducers) are affected by the environmental variations and each sensor's limitations [25]. In general, *in-situ* calibration procedures must include a mechanism to identify what exogenous parameters should be included in the pollutant estimation model. The criterion may combine meteorological information [32], [42] or introduce heuristics such as timestamps [36] (see Table 1). As a result, we consider that taking advantage of the environmental dynamics may improve the accuracy of the estimations. For this reason, this work proposes a combination of meteorological information and heuristics, in addition to a decision rule to find an optimal combination of sensors for the estimation model.

B. RELATED WORK

As initially stated in the previous section, the reliability of a RAMP monitor depends on the calibration methods used to adjust the measurements of low-cost sensors. It is a common practice for evaluating the quality of the estimation models, the use of statistical parameters, such as the coefficient of correlation (r) and the root mean square error (*rmse*) between a reference and the actual estimation on an hourly basis. The reference value is obtained from official fixed air monitoring (FAM) stations that comply with the recommendations of the United States Environmental Protection Agency (US EPA) and/or the Data Quality Objectives (DQO) of the European Commission.

Several commercial platforms have been used in the past (Aeroqual and AQmesh) to evaluate estimation models, and the most common low-cost sensor technology company seems to be Alphasense (see Table 2). However, there are almost no evaluations of the MQx family sensors from Hanwei and Winsen. Such sensors and modules have a lower cost ranging from 2 to 25 USD, and have been chosen in this project. In the case of [37], the calibration of multiple ozone and carbon monoxide sensors in a semi-urban area resulted in a strong relationship between the values of the reference station and the RAMP station (with models including temperature corrections, relative humidity and aging of the device).

TABLE 2. Performance in field calibration: O_3 estimation.

System	r	Sensor / Platform
Moltchanov et al, 2015 [43]	0.88 - 0.97	Aeroqual SM50
Spinelle et al, 2015 [26]	0.90 - 0.94	The Citytech O3 3E1F
Lin et al, 2015 [44]	0.95	Aeroqual S500
Borrego et al, 2016 [45]	0.36 - 0.84	Alphasense O3-B4
Jiao et al, 2016 [37]	0.90 - 0.97	Aeroqual SM50
Castell et al, 2017 [24]	0.10 - 0.81	Alphasense OX-B421
Pang et al, 2018 [40]	0.94	Alphasense OX-B421
Topalović et al, 2019 [41]	0.38 - 0.88	AQMesh

The Pearson coefficient in the best case reached 0.97 and 0.82, respectively; however, the cost of the station proposed by [37] is around 2,000 USD per pollutant (6.6 times the maximum cost of the station for this project, which could be expensive for developing countries).

Research platforms sensing ozone and evaluated in the last four years are presented in Table 2. Similarly, Table 3 shows the correlation between carbon monoxide estimations and official fixed air monitoring stations in recent systems. However, the actual accuracy may diminish with time as the model may not include the signal drift and aging of the low-cost sensors. Moreover, in some works additional measurements are used to generate specific models for certain environmental considerations. For instance, [33] evaluates and compares metal-oxide sensors and electro-chemical sensors with linear and nonlinear regression techniques for ozone estimation; however, the seasonal appearance of ozone in summer and meteorological variations may require different calibration models for other seasons and pollutants, reducing the accuracy in results from extrapolated values (i.e. lower temperatures from winter).

TABLE 3. Performance in field calibration: *CO* estimation.

System	r	Sensor / Platform
Borrego et al, 2016 [45]	0.73 - 0.93	Alphasense CO-B4
Jiao et al, 2016 [37]	0.79 - 0.82	AQMesh
Spinelle et al, 2017 [27]	0.15 - 0.60	TGS5042
Castell et al, 2017 [24]	0.58	AQMesh
Spinelle et al, 2017 [27]	0.87 - 0.88	MICS-4514
Topalović et al, 2019 [41]	0.62 - 0.91	AQMesh

In the case of [32], a 6-months experiment compared MLR and RF models to estimate several pollutant concentrations with multiple RAMP monitors. As result, the RF approach outperformed the classical MLR. However, the calibration and evaluation sets were part of the same time frame. More specifically, the training set may have included data from the beginning, the middle and the end of experiment, in order to have enough variations in data which improve the performance of models. From our point of view, this evaluation was not realistic, and may not represent the true performance of estimation models in the RAMP monitor in a new time frame, where other environmental conditions are found. In addition, a comparison of RF and ANN-MLP would be of importance for decision making in the calibration process of RAMP monitors working in real scenarios. Therefore, we analyze and compare these two methods in this research.

In [42], the calibration of MLR models for O_3 and NO_2 estimation is implemented with the help of three correction factors: temperature, humidity and wind-speed. They propose an environment-adaptive continuous calibration scheme with a distributed model. Although the proposal is attractive, the error due to signal drift may be considerable in a network of RAMP monitors with different aging, specially with metal-oxide CO_x sensors.

Recent works have shown that including meteorological and multi-pollutant data in the same system improves the accuracy of RAMP monitors. In Table 1, several calibration techniques, mostly based on machine learning algorithms, include other pollutants information, as well as other variables such as temperature, humidity, atmospheric pressure and aging. This is intended to correct cross-sensitivity and environmental effects on sensors. However, the selection of the ideal combination of sensors is usually based on a decision rule that considers a threshold in the coefficient of correlation between the reference and the each sensor [26], [41]. This may not consider the overall performance and the actual error, more specifically, the *rmse*. In other cases [32], [37], the calibration model includes both temperature and humidity, which are directly related and inversely correlated. However, this may add noise to the calibrated model. As a result, we suggest that a better way to select the sensor combination would be by considering r and *rmse* in the decision rule.

To date, several long-term evaluations have been carried out in places with relative strong meteorological variations, resulting in the aggregation of variables for seasonal considerations. Therefore, we propose to perform an experiment near the Equator, in which the temperature and humidity do not vary considerably during the year, focusing the project on selecting an optimal sensor combination and calibration algorithm that minimizes the estimation error in outdoors operation.

III. EXPERIMENTAL SYSTEM ARCHITECTURE

This section describes in detail the practical considerations of the experiment such as geographical location, reference equipment, hardware components (e.g. sensors, processing devices and instrumentation) and software packages (e.g. programming language and libraries) powering the RAMP monitor. With this setup we have generated the data sets to evaluate the estimation models as well as the methodology of heuristics and sensor selection proposed in this work.

The experimental system architecture (see Fig. 1) is composed by three elements: the RAMP monitor, the FAM station and a remote displaying/control device. All three devices have network access. The low-cost air composition monitor integrates IEEE 802.3 and IEEE 802.11 connectivity, allowing full remote access to upload new calibrated models, access to the stored data, modify services and routines, and

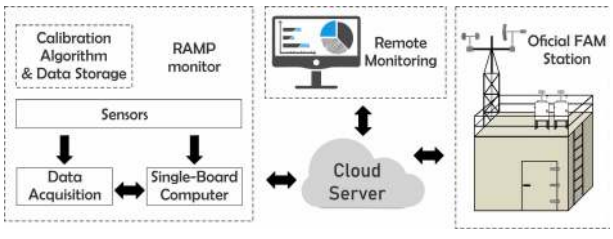

FIGURE 1. Experimental system architecture.

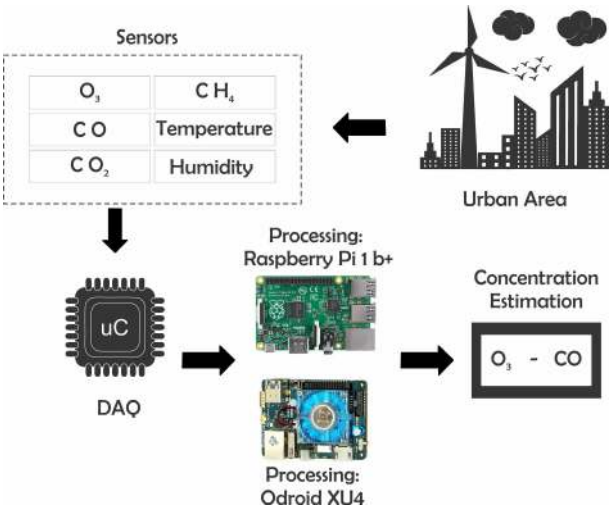

FIGURE 2. Architecture of the RAMP monitor.

FIGURE 3. Sensors in the RAMP monitor.

to test the system response in a real environment. In addition, the FAM station integrates Ethernet connectivity as well, and the data can be accessed through a web service. The displaying/control device is a computer that receives the information from the other two elements upon request, and can interact with the RAMP monitor.

A. RAMP MONITOR

Fig. 2 shows the general scheme of the prototype. This device combines several off-the-shelf hardware. The description of the prototype components is detailed below:

- Processing devices. The prototype architecture includes two single-board computers that receive information from the sensors using digital communication or through a serial interface with a data acquisition board (DAQ). The first monitor is a Raspberry Pi 1 b + (RPI b +), with Raspbian Stretch operating system. The second monitor is an Odroid XU4 (O-XU4), with Ubuntu Mate operating system. Both are connected to a MySQL database to store the information. In addition, a background service is executed in each operating system, scheduled to collect the samples from the sensors once per second. These two computers are working simultaneously for redundancy, since we have no physical access to the location of the RAMP monitor after the installation. If one device fails, the other may continue storing the data.
- Data acquisition card. The DAQ uses the Microchip PIC 18F25k50 microcontroller, which records 4 analog channels.
- Sensors. The sensors (see Fig. 3) connected to each computer are shown in the Tables 4 and 5. With the intention of generating redundancy, several sensors of the same type have been installed together with other gas sensors. Having several sensors for different pollutants helps to reduce cross-sensitivity during the calibration; more specifically, the models may learn to adjust the estimated values of the target pollutant when other pollutants affect the measurement in the sensor. The prototype uses three carbon monoxide sensors, two of them from the Spec Sensors brand (model DGS-CO 968-034, SPEC CO) with digital outputs and values in the range of 0− 1000 *ppm*, while the other Hanwei MQ-7 sensor has an analog readout with an operating range of 10 − 10,000 *ppm* and connects to the DAQ. To estimate the ozone concentration, two Winsen brand MQ-131 sensors are used, one with plastic hooded (for low concentrations, range between 0.01 − 1.00 *ppm*) connected to the RPI b + and the other with metallic hooded (for high concentrations, range between 10 − 1000 *ppm*) connected to the O-XU4. Details on the operating ranges of each sensor are shown in Table 6.
- Protective case. To protect the electronic components from environmental conditions, a galvanized metal

TABLE 4. Monitor - Raspberry Pi 1 b+.

Sensor	Measurement	Data	Connection
SPEC CO - Spec Sensors	CO	Serial	RPI b+
MQ-131 - Plastic Cap (P)	O_3	ADC -10 bits	DAQ
BMP280 - BOSH	T	I2C	RPI b+
SPEC CO - Spec Sensors	RH	Serial	RPI b+

Note 1: T —temperature, RH —relative humidity.

TABLE 5. Monitor - Odroid XU4.

Sensor	Measurement	Data	Connection
SPEC CO - Spec Sensors	CO	Serial	O-XU4
MG-811 - SEN0159	CO_2	ADC - 10 bits	DAQ
MQ-4 - Module	CH_4	ADC - 10 bits	DAQ
MQ-7 - Module	CO	ADC - 10 bits	DAQ
MQ-131 - Metallic Cap (M)	O_3	SPI	DAQ
Si7021-A20	T	I2C	O-XU4
Si7021-A20	RH	I2C	O-XU4

Note 1: T —temperature, RH —relative humidity.

TABLE 6. Operational range of sensors.

Sensor	Measurement	Range
SPEC CO	CO	$0 - 1000\ ppm$
MQ-7	CO	$10 - 10000\ ppm$
MG-811	CO_2	$400 - 10000\ ppm$
MQ-131 (P)	O_3	$0.01 - 1.00\ ppm$
MQ-131 (M)	O_3	$10 - 1000\ ppm$
MQ-4	CH_4	$200 - 10000\ ppm$
BMP280	T	$-40 - 85°C$ ⋆
Si7021-A20	RH	$0 - 80\%$ ⋆
Si7021-A20	T	$-10 - 85°C$ ⋆

Note 1: T —temperature, RH —relative humidity.
⋆ Recommended operational range.

protective cover was used. The structure is waterproof, and the enclosure is open at the bottom to allow the air to enter the case. The dimensions (length, width and thickness) are $30 \times 22 \times 6$; *cm* (Fig. 4).

FIGURE 4. RAMP monitor.

B. REFERENCE STATION

The reference data utilized for the calibration and evaluation of this work was obtained from an official fixed air quality monitoring station located near by the main square of the city of Cuenca – Ecuador. This station is owned by EMOV EP, the municipality entity regulating the mobility, traffic and transportation. This station has analyzers of O_3, CO, NO_2, SO_2 and $PM_{2.5}$. In addition, it measures meteorological parameters such as temperature, relative humidity, wind speed, barometric pressure, solar radiation and precipitation. These values are collected, evaluated and published annually [46]. For the purpose of this research, only the data from the analyzers of ozone and carbon monoxide are considered; the other values are not used throughout this work. The FAM station has an ultraviolet photometry analyzer of brand/model Teledyne M400E (see Fig. 5) that uses Beer-Lambert law applied to ultra violet light to estimate the concentration of ozone in a chamber. The other analyzer is a Teledyne M300E (see Fig. 6) that measures the concentration of carbon monoxide with the nondispersive infrared radiation method. Both of the analyzers comply with the recommendations of the US EPA with equivalent method EQOA-0992-087 [47], [48], and are periodically calibrated against reference to

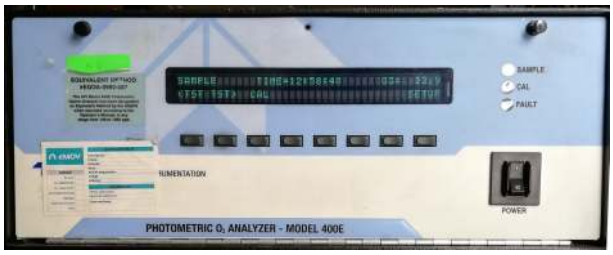

FIGURE 5. Reference monitor for ozone: Teledyne M400E.

FIGURE 6. Reference monitor for carbon monoxide: Teledyne M300E.

maintain its accuracy. The sampling time of the equipment is 1 minute. More information of the FAM station can be found in [46].

Since the objective is to generate bivariate data sets of the same environment, the RAMP monitor was positioned alongside the reference instruments. More specifically, next to the air duct that connects with the sampling tube of the FAM station, as shown in Fig 7.

FIGURE 7. Location of RAMP monitor in the FAM station.

Even though the FAM station and the RAMP monitor measures pollutant concentrations with a period of 1 minute and 1 second, respectively, this research considers hourly averages of pollutant concentrations in the evaluation of the methodology, hereafter. We only use hourly indicators given that several air quality concentration standards

show the effects scale of Carbon Monoxide on hourly averages [11], [12].

IV. VALIDATION METHODOLOGY & ANALYSIS

A. DATA MEASUREMENT CAMPAIGN

Data acquisition from the FAM was executed from July 20^{th}, 2019 to October 17^{th}, 2019. The data stored in each processing unit in the RAMP monitor was synchronized during the whole experiment. This can be verified by observing the timestamps and the variations in temperature and humidity in each processing unit. For instance, Fig. 8 shows the synchronized values obtained from the temperature and humidity sensors connected to the RPI 1 b+ and Odroid XU4 during the first 14 days.

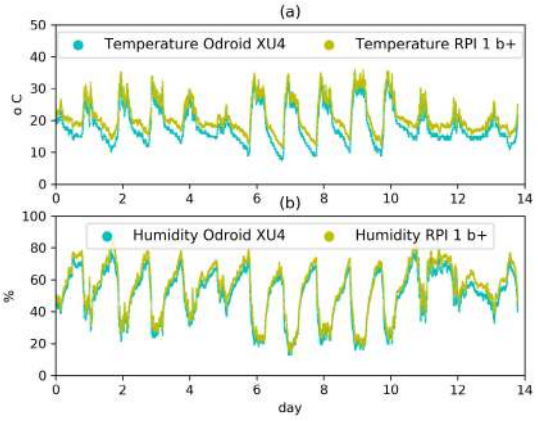

FIGURE 8. Synchronized values of temperature (a) and humidity (b) in each processing unit.

As proposed initially, the data was divided into two sets: calibration set (CS) and evaluation set (ES). Each set was used to implement and evaluate the three estimation models: multiple linear regression, artificial neural network and random forest.

- Calibration set (CS). The data generated during the first thirty days of operation was used to calibrate the estimation models. This period includes the summer break at Cuenca, Ecuador, in which traffic decreases, resulting in lower pollutant concentrations.
- Evaluation set (ES). The data collected during the next 58 days was used to evaluate the calibrated models: the last days of August, the month of September and the first seventeen days of October. Traffic increases in September due to the start of academic period in schools and universities. In consequence, pollutant concentrations are usually higher in the beginning of September, which challenges the performance of models in scenarios with different dynamics and higher concentrations. In particular, during July and August 2017 the concentration of ozone had its peak at ∼40 *ppb* with 8-hour averages; however, during September, this pollutant reached 56 *ppb* [46].

B. STATISTICAL TOOLS

To determine the accuracy of the estimation of pollutant concentrations, some statistical tools are used in order to compare this work with previous research, while additional parameters help to understand the operational considerations of this work. The statistical analysis of the following sections uses the reference data (y_r) and the estimated value (y_e). This produces a bivariate set of ordered pairs $(y_{r-i}, y_{e-i})\ \forall\ i = 1, 2, 3, .., n$, where n is the sample size. The mean value of y_r and y_e are $\bar{y}_r$ and $\bar{y}_e$, respectively. The metrics used throughout document are:

- Coefficient of Correlation (r). It is used to establish a level of association between the reference value and the estimated value. The range of the correlation is $[-1,1]$; higher values of the absolute value of r represents better calibrated models to resemble the reference. If the calibration algorithm that estimates the concentration of the pollutants results in a correlation of 1 with the reference, then the bivariate would be proportional, satisfying the condition $y_{r-i} = ky_{e-i}$ where $k\ \varepsilon\ \mathbb{R}$.

$$r = corr(y_e, y_r) \tag{1}$$

$$r = \frac{\sum_{i=1}^{n} y_{e-i}y_{r-i} - n\bar{y}_{e-i}\bar{y}_{r-i}}{\sqrt{\sum_{i=1}^{n} y_{e-i}^2 - n\bar{y}_e}\sqrt{\sum_{i=1}^{n} y_{r-i}^2 - n\bar{y}_r}} \tag{2}$$

- Bias (be) or Mean Error. The bias error is the average error from a given set, as in (3):

$$be = \sum_{i=1}^{n} \frac{y_{r-i} - y_{e-i}}{n} \tag{3}$$

- Mean Absolute Error (mae). The mean absolute error is an indicator of disagreement between y_r and y_e. This is obtained with (4).

$$mae = \sum_{i=1}^{n} \frac{|y_{r-i} - y_{e-i}|}{n} \tag{4}$$

- Root Mean Squared Error ($rmse$). The mean squared error (mse) is a metric for the goodness of the estimator that includes the uncertainty of the estimation process. It is a non-negative value, and it becomes the variance of the error for unbiased data. However, to use a metric with the same units of the estimator, the root of the mse is obtained instead, as presented in (5).

$$rmse = \sqrt{\sum_{i=1}^{n} \frac{(y_{r-i} - y_{e-i})^2}{n}} \tag{5}$$

- Uncertainty (U). In order to calculate the margin of the estimation error, we propose a confidence level of 95% ($\alpha = 0.05$). Then, the confidence interval of the error can be expressed as:

$$c.i. = be \pm 1.96\sigma_e^2 \tag{6}$$

where σ_e is the standard deviation. Additionally, the range of operation (OR) is obtained as follows:

$$OR = max(y_{r-i}) - min(y_{r-i}) \tag{7}$$

then, the uncertainty U in percentage is:

$$U = \frac{max(|be \pm 1.96\sigma_e^2|)}{OR} \times 100\% \quad (8)$$

C. DATA ANALYSIS

The variations of temperature and relative humidity have an important relationship in the calibration. This is observable in the correlations of each sensor, analyzed during the first thirty days of operation, detailed in Table 7. In general, there is a positive correlation between the sensors and the temperature, while there is a negative correlation between the sensors and the relative humidity. For this reason, it is important to introduce the temperature and relative humidity measurements in the calibration model. During the experiment, the temperature and humidity oscillated between $7°C - 38°C$ and $9\% - 85\%$, respectively. In addition, the methane sensor (MQ-4) was ignored, since its values were negligible ($\sim$0 during the measuring campaign).

TABLE 7. Coefficient of correlation: sensors vs. temperature & humidity.

Sensor, Monitor	Temperature	Humidity
MQ-7, O-XU4 (CO)	0.55	-0.48
MQ-131 (M), O-XU4 (O_3)	0.15	0.01
MG-811, O-XU4 (CO_2)	0.06	0.00
SPEC CO, O-XU4 (CO)	0.89	-0.79
SPEC CO, RPI b+ (CO)	0.90	-0.81
MQ-131 (P), RPI b+ (O_3)	0.58	-0.43

The reference values together with the normalized and unprocessed measurements of the CO sensors (between day three and four) and O_3 (between day seven and eight) are shown in Figures 9 and 10. It is possible to observe the temperature pattern embodied in the analog reading of the sensors. In addition, the strong positive correlation between temperature and measurement is notable, especially in the SPEC CO modules with $r \sim 0.90$. On the other hand, when analyzing the cross-correlation between sensors presented in Table 8, there seems to be an almost insignificant relation

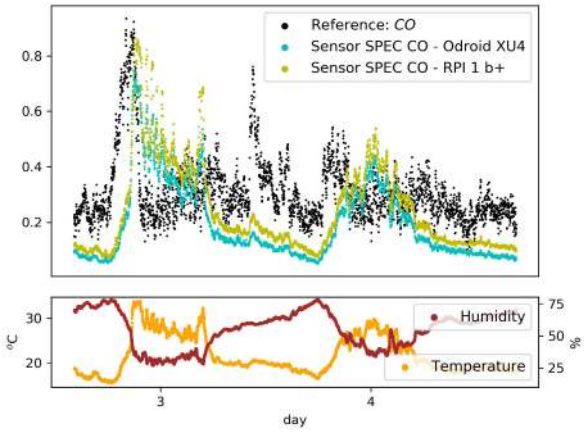

FIGURE 9. Normalized values of carbon monoxide.

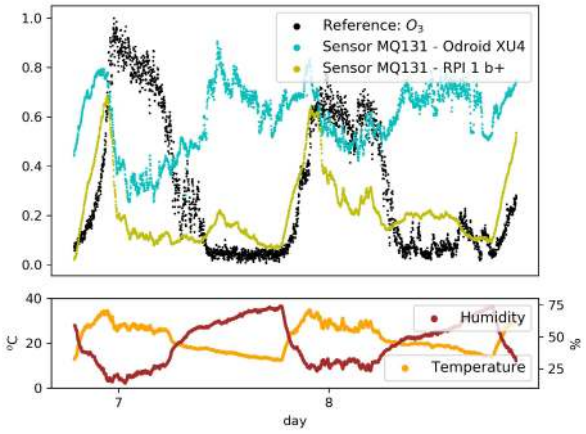

FIGURE 10. Normalized values of ozone.

TABLE 8. Coefficient of correlation: between sensors.

Sensors	SPEC CO	MQ-7	MG-811	MQ-131 (P)	MQ-131 (M)
SPEC CO	1.00	-	-	-	-
MQ-7	0.67	1.00	-	-	-
MG-811	-0.09	0.09	1.00	-	-
MQ-131 (P)	0.47	0.22	0.63	1.00	-
MQ-131 (M)	0.35	0.26	0.09	0.48	1.00

between CO_x sensors. However, when evaluating the correlation during the campaign, such relation increases considerably. This will be shown in the results.

V. CALIBRATION METHODOLOGY

A. SENSOR COMBINATION

In order to find the optimal combination of sensors in the calibrated model, we propose a decision rule as follows:

- First, we aim to maximize r. This means that the model with the highest correlation may lead best fit. However, high correlation doesn't imply low error. For instance, this is the case of signal drifting in some sensors due to aging.
- Second, we expect the model to have the lowest *rmse*. The estimation error is aimed to be as low as possible (minimize *rmse*).
- Third, the decision rule to select the optimal combination of sensors involving correlation and the error solves the maximization problem shown in (9), which will be the performance index of the model:
  Find a set of sensors $x_j, x_k, \ldots, x_m \; \forall j \neq k \leq n$ where n is the number of available sensors, such that:

$$f(x_j, x_k, \ldots, x_m) \Rightarrow max\left(\frac{corr(y_r, y_e)}{rmse(y_r, y_e)}\right) \quad (9)$$

where $f(x_j, x_k, \ldots, x_m)$ is the estimation model, $rmse > 0$ and $-1 \leq corr(y_r, y_e) \leq 1$

As shown in (9), the optimal sensor combination can be evaluated using a function that has m independent variables. For simplicity, the function $f(x_j, x_k, \ldots, x_m)$ implements Multiple Linear Regression to evaluate each tuple of

sensors, and, in general, for any regression model, f becomes the estimated output such that $f(x_j, x_k, \ldots, x_m) = y_e$.

This process (see Fig. 11) uses the calibration set, and divides it into two subsets: first subset (SSC) contains the data collected between the 1^{st} and the 15^{th}, and the second subset (SSE) consists of the data collected between the 16^{th} and the 30^{th} day. The SSC is used to solve the regression problem, while the SSE is used for evaluation and calculation of the performance index. These two subsets are selected to include the sensor variations due to the aging process during the first month. For this reason, the SSE evaluation is aim to find and discard sensors with a negative impact in the performance for a long term perspective. As a result, after evaluating all the possible combinations of the sensors and each performance index, the optimal tuple to estimate ozone and carbon monoxide concentrations are:

$$O_3 \Rightarrow (MQ - 131_M, MQ - 131_P, SPEC\ CO, T) \quad (10)$$

$$CO \Rightarrow (MG - 811, MQ - 7, MQ - 131_M, RH) \quad (11)$$

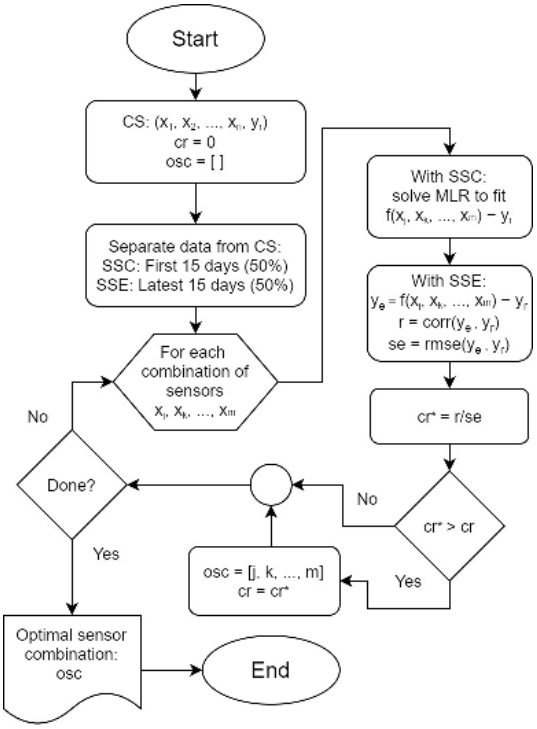

FIGURE 11. Flowchart to find an optimal sensor combination.

The python library used to obtain the model and evaluate each sensor combination is scikit-learn [49].

In addition to the optimal sensors combination, we propose to add a heuristic (timestamp) as another input in the estimation model. It may become useful since we found that in general, the daily concentrations are very similar between each other[1] (see Fig. 12).

[1]This approach may be applied in places where the meteorological conditions and seasonality are similar to the conditions present in the city of Cuenca. Near the Equator, the temperature and humidity do not change drastically throughout the year.

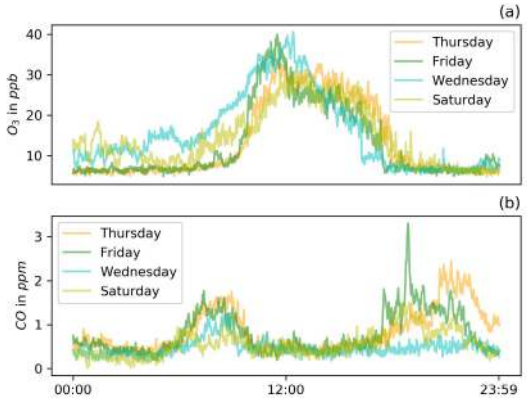

FIGURE 12. Similarities in daily concentrations of O_3 (a) and CO (b). Week II.

This idea was analyzed by comparing the concentrations per minute of ozone and carbon monoxide of several days. In Fig. 13 and Fig. 14, the black dashed line represents the ideal association between the samples, and it is possible to observe that relation between the concentrations of several days is not a perfect line, but it does present a pattern that could be learned by the estimation model, specially for ozone concentrations. As a result, temporal information may be

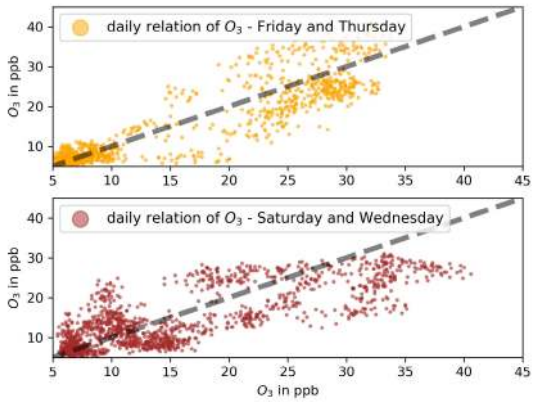

FIGURE 13. Similarities in O_3 concentrations between several days. Week II.

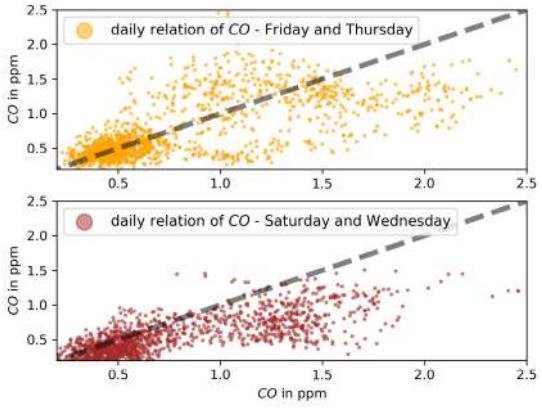

FIGURE 14. Similarities in CO concentrations between several days. Week II.

considered as a heuristic to improve accuracy, since higher concentrations are expected at a certain time of the day. The heuristic is of importance, specifically for non-linear models that may learn patterns of daily concentrations on a hourly basis. This approach may have an important impact, specially when it is needed to deploy a network of RAMP monitors in a urban area with similar environmental dynamics. To illustrate this concept, let us consider a-priori information of the pollutant concentrations as in Fig. 15. Two distributions are shown for each pollutant at different hours; given that higher concentrations are expected a certain time (11 am and 8 am for ozone and carbon monoxide, respectively), we include the time of the day in the estimation model, so it can learn that higher concentrations are usually related to specific hours of the day. In other words, if the distributions of the pollutant concentrations are known on an hourly basis, then it may be included in the model.

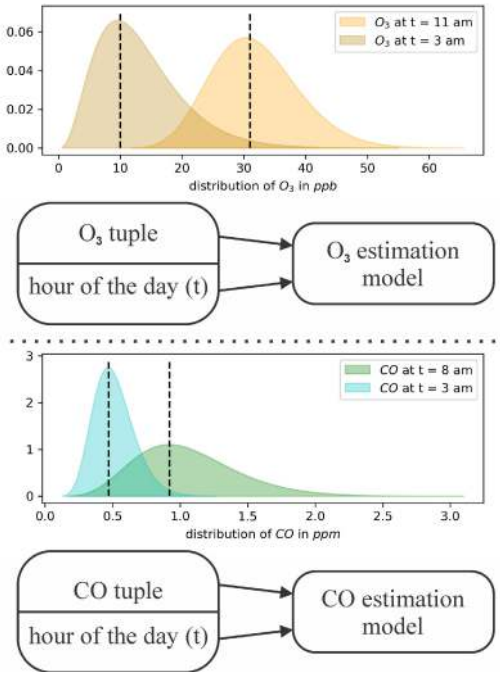

FIGURE 15. The hour of the day is associated with the pollutant concentrations.

B. CALIBRATION METHODOLOGY

Three calibration methodologies are evaluated: multiple linear regression, artificial neural networks and random forest. Each methodology implements 8-fold cross-validation strategy with the data obtained during the first thirty days of operation, and by using (9) as the decision rule to select the optimal model. More specifically, the CS is divided in 8 different subsets (12.5 % of CS), and the regression algorithm is implemented in each subset and evaluated in the remaining subsets (87.5 % of CS). The resulting models require five inputs, which are the sensors described in 10 and 11 and the timestamp. The calibration methodology is the same for both pollutants of interest.

1) MULTIPLE LINEAR REGRESSION

One of the most used regression models for prediction is the MLR. Given a set of reference points y_{r-i} points for $i = 1, 2, 3, \ldots, n$ and each point is associated to a set of m independent variables $X = x_{1-i}, x_{2-i}, x_{3-i}, \ldots, x_{m-i}$. Then, it is possible to implement a multiple linear function y_{e-i} such that:

$$y_{e-i} \sim y_{r-i} = \beta_0 + \beta x_{1-i} + \beta x_{2-i} + \ldots + \beta x_{m-i} + \epsilon \quad (12)$$

where ϵ = random error and $\beta = \beta_0, \beta_1, \ldots, \beta_m$ = constant coefficients.

In matrix form:

$$Y_r = \beta X + \epsilon \quad (13)$$

Applying ordinary least squares to Y_r, the optimal estimator of β^* is:

$$\beta^* = (X^T X)^{-1}(X^T Y_r) + \epsilon \quad (14)$$

Then, the resulting model used to evaluate the performance index is:

$$Y_e = \beta^* X + \epsilon \quad (15)$$

2) MULTIPLE LAYER PERCEPTRON

In artificial neural networks (ANN), the MLP is an architecture composed of three or more layers (see Fig. 16). The input layer has at least one node, each node representing a measurement of the environment. In addition, there are hidden fully interconnected layers with neurons and an output layer with a single neuron estimating the actual concentration. The hidden and the output layers are composed of neurons associated to activation functions. The training algorithm is the *root mean squared propagation* (RMSprop) with the least squares criterion. The configuration for both of the models is shown in Table 9. The python library used to implement this architecture is *Pytorch* [50].

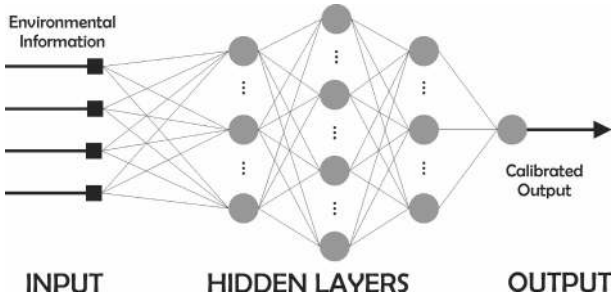

FIGURE 16. MLP-ANN architecture.

3) RANDOM FOREST

This method can be used for classification and regression problems. It creates subsets from a sampling space, and produces multiple decision trees to model complex relationships (see Fig. 17). Each decision tree uses environmental information to estimate the best outcome by averaging

TABLE 9. Detail of the layers - MLP neural network.

Layer	# Connections	Activation Function
Input	5	ReLU
Hidden 1	24	ReLU
Hidden 2	12	ReLU
Output	1	Lineal

Note 1: ReLU - rectified linear unit

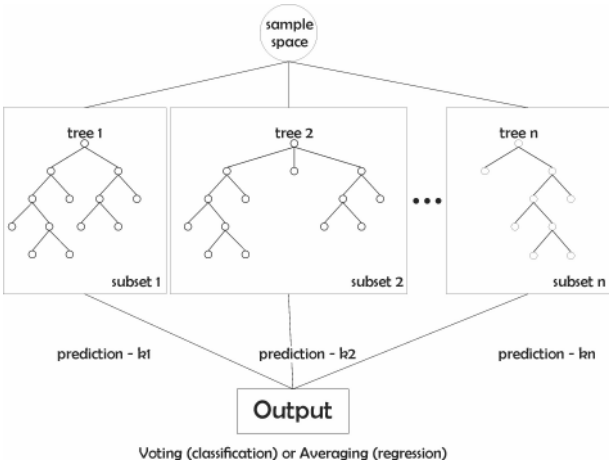

FIGURE 17. RF architecture.

(regression task). In addition, the algorithm is stable and prevents data over-fitting, however, it might not extrapolate with the required accuracy if the system presents relative strong dynamics. Moreover, computational power is compromised as the number of expansion trees grows. Both models (ozone and carbon monoxide) are implemented with 10 trees, and the python library used to evaluate this method is scikit-learn [49].

VI. RESULTS

The estimation models for ozone and carbon monoxide are evaluated independently in this section, and the results are organized as follows:

- First, comparative dispersion plots of reference vs estimation for each calibration method are presented, considering the CS and ES independently.
- Secondly, the performance metrics: *be*, *mae*, *rmse* and *r* are shown. Moreover, modified Taylor diagrams presenting the daily *rmse* and *r* corroborate the metrics from a visual perspective. The diagram shows the performance metrics mapped in a quadrant of the Cartesian plane: the closer the dots are to the origin, the lower the value of *rmse*. Similarly, the closer the diamonds are to the horizontal axis, the higher the correlation.
- Thirdly, a five-days plot within the evaluation period show the actual estimation with lower and upper limits considering 30 % and 25 % of relative uncertainty for ozone and carbon monoxide, respectively.

As a reference for the values shown in this section, the US EPA and the Air Quality Index (AQI) model categories presents the range of ideal pollutant concentrations (8-hour averages, 1st category - good air quality index) [12]: $O_3 < 54$ *ppb* and $CO < 4.4$ *ppm*.

A. OZONE ESTIMATION MODELS

From the three estimation models, Fig. 18 (a) shows that RF has an almost ideal assessment during the calibration process; however, this ideal behavior vanishes during the evaluation (see Fig. 18 (b)). In fact, the initial slope (m) of the trending line of the bivariate data is 0.98 and drops to 0.77 with ES, and the interception (b_o) increases from 0.44 *ppb* to 4.44 *ppb* (see Table 10). This may be seen as an over-trained model; yet several experiments with various parameters (*i.e.* different number of trees) and calibration sets lead to similar results. It is important to mention that other several experiments with RF and an unique time frame lead to better and more consistent results (similar to the methodology and results described in [32]) with the ES; however, that approach is not realistic and separated time frames should be used.

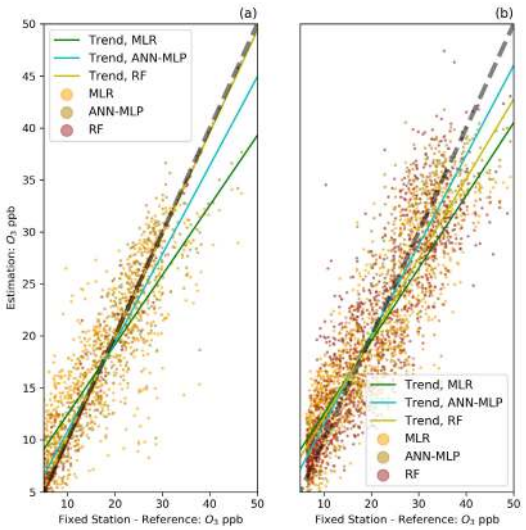

FIGURE 18. Trending line in O_3 estimation models with CS (a) and ES (b).

TABLE 10. Trending line values - O_3 estimation.

Method	b_o - CS	m - CS	b_o - ES	m - ES
Multiple Linear Regression	5.74	0.67	5.53	0.70
Artificial Neural Network	2.31	0.85	2.83	0.86
Random Forest	0.44	0.98	4.44	0.77

On the other hand, more consistent results are found with the MLP-ANN model: the performance in terms of *r* and *rmse* decrease in less than 1.1 % and 1 *ppb*, respectively. In addition, the interception of the trending line is at least 37 % smaller than MLR and RF, resulting in the best estimation technique. Moreover, with the same method the estimation error during the two-months evaluation period (ES) resulted in an overall uncertainty of 16 %; more specifically, for each sample tuple the estimation error was $\leq$8.2 *ppb* with

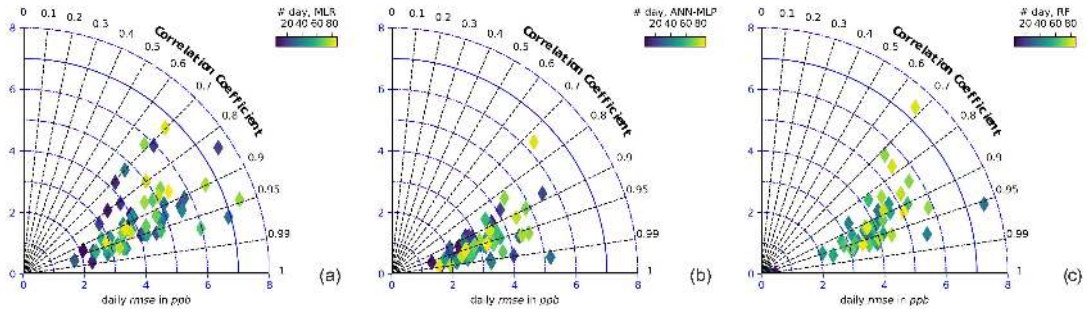

FIGURE 19. Modified Taylor diagram for O_3 estimation models by using (a) MLR; (b) ANN-MLP; and (c) RF.

95 % of confidence. During the three-months experiment, the minimum and maximum concentrations of ozone were 3.5 *ppb* and 55.5 *ppb*, respectively, which shows a good air quality at the evaluation place. However, the performance evaluation is limited to this pollutant concentration range.

The performance metrics are shown in Tables 11 - 14. In general, ANN-MLP present the best performance during the evaluation period: lowest *be*, *mae*, *rmse* and highest *r*. In despite of good performance with the RF model during the calibration period, it doesn't seem to estimate with the same accuracy under different meteorological conditions.

TABLE 11. Bias error in *ppb*.

Method	O_3 - CS	O_3 - ES
Multiple Linear Regression	-0.19	0.76
Artificial Neural Networks	0.17	0.02
Random Forest	-0.08	0.44

TABLE 12. Mean absolute error in *ppb*.

Method	O_3 - CS	O_3 - ES
Multiple Linear Regression	4.00	4.14
Artificial Neural Networks	2.52	3.26
Random Forest	0.33	3.89

TABLE 13. Root mean squared error in *ppb*.

Method	O_3 - CS	O_3 - ES
Multiple Linear Regression	5.23	5.08
Artificial Neural Networks	3.34	4.17
Random Forest	0.99	5.05

TABLE 14. Coefficient of correlation.

Method	O_3 - CS	O_3 - ES
Multiple Linear Regression	0.81	0.88
Artificial Neural Networks	0.93	0.92
Random Forest	0.99	0.88

Even though the daily results of the MLR approach presented in Fig. 19 (a) are stable during the campaign, Fig. 19 (b) presents a higher concentration of diamonds in the lower left side of the modified Taylor diagram for the ANN-MLR model, with the exception of one outlier almost at the end of the experiment (*rmse*∼6.2 and *r*∼0.73). However, for the rest of the experiment, the performance of the model with the ES and CS are mixed in the same space. In contrast, the RF model has a high concentration of diamonds at the origin (see Fig. 19 (c)) with the CS; yet the performance decreased at least in 2 *ppb* starting from the 31^{st} day, corroborating the difference in the effectiveness between two different time frames for the RF model. Moreover,

An example of the estimation of ozone during days 60 to 65 is shown in Fig. 20. The estimation models are very close to the reference values of the official FAM, and most of the estimations are within the upper and lower limits of relative uncertainty.

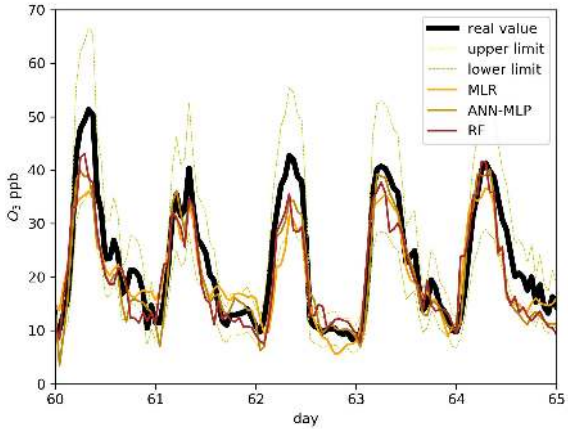

FIGURE 20. Experimental results, O_3 estimation models and relative lower and upper uncertainty boundaries.

B. CARBON MONOXIDE ESTIMATION MODELS

In the estimation of Carbon Monoxide, the concentrations oscillated between 0.00 *ppm* and 2.83 *ppm*, and the results where no significantly different with the ES in the three *CO* models of this work. However, several considerations arose during the training and evaluation process.

The QoI during the training of the models was ideal with the RF approach; yet, the evaluation demonstrated a different

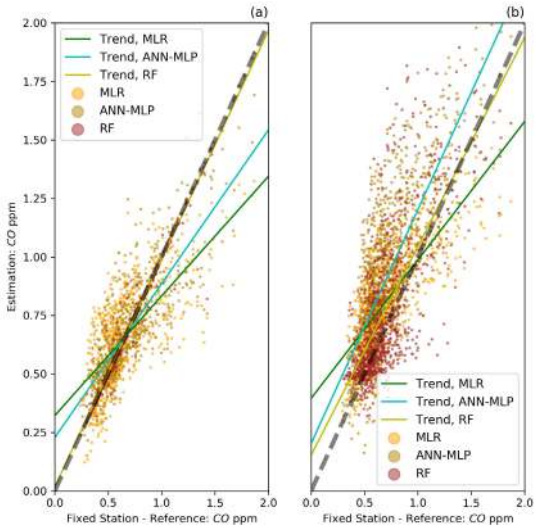

FIGURE 21. Trending line in *CO* estimation models with CS (a) and ES (b).

TABLE 15. Trending line values - *CO* estimation.

Method	b_o - CS	m - CS	b_o - ES	m - ES
Multiple Linear Regression	0.32	0.51	0.40	0.59
Artificial Neural Network	0.23	0.65	0.20	1.00
Random Forest	0.01	0.97	0.15	0.89

perspective. This can be observed in the scatter plots of Fig. 21 (a) and (b) together with the values of slope (m) and interception (b_o) of the trending lines shown in Table 15. It is important to mention that the estimations with the RF model have a great fit (see Fig 21 (a)) only with the CS. Then, the data dispersion with the ES (see Fig. 21 (b)) shows a growing vertical relation in low concentrations of carbon monoxide, resulting in misleading higher estimations in all the models. In despite of the dispersion differences between the estimations with the ES and CS, the slope of the RF approach has smallest variation between the CS and ES. On the other hand, even tough the ideal $m = 1$ with the ANN-MLP approach, there is a vertical shift of the trending line for this model, resulting in higher values of *rmse*.

According to the metrics shown in Tables 16 - 19, the best results in the ES are from the Multiple Linear Regression model, considering (9) in the three approaches. In addition, unexpectedly, this model had a lower *rmse* with the pass of the days (see Fig. 22). In contrast, the performance in the ANN-MLP model decreased as the metal-oxide sensors aged. Subsequently, the two latest months of this experiment resulted in an overall uncertainty of 16 % in the MLR estimation model and an error <0.44 *ppm* with 95 % of confidence.

TABLE 16. Bias error in *ppm*.

Method	CO - CS	CO - ES
Multiple Linear Regression	0.00	-0.11
Artificial Neural Networks	0.00	-0.20
Random Forest	0.00	-0.08

TABLE 17. Mean absolute error in *ppm*.

Method	CO - CS	CO - ES
Multiple Linear Regression	0.15	0.16
Artificial Neural Networks	0.12	0.23
Random Forest	0.01	0.16

TABLE 18. Root mean squared error in *ppm*.

Method	CO - CS	CO - ES
Multiple Linear Regression	0.20	0.17
Artificial Neural Networks	0.15	0.21
Random Forest	0.04	0.20

TABLE 19. Coefficient of correlation.

Method	CO - CS	CO - ES
Multiple Linear Regression	0.71	0.75
Artificial Neural Networks	0.83	0.76
Random Forest	0.99	0.74

An important concern of the CO_x metal-oxide sensors arose with the signal drift due to aging, harsh environment and cross-sensitivity. During this experiment, the variations

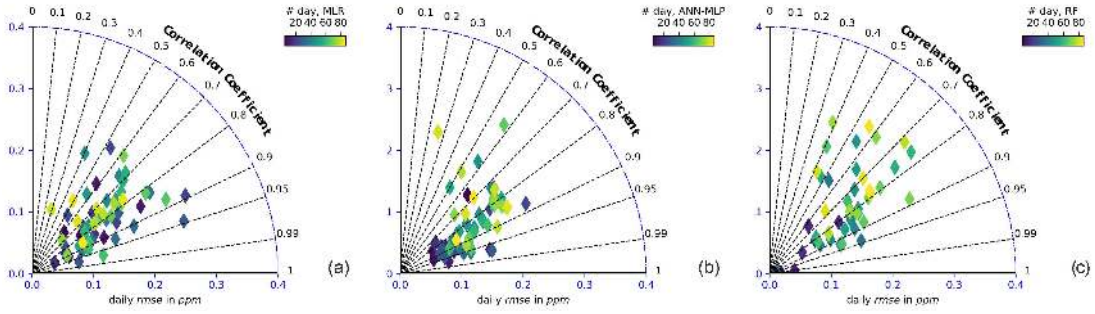

FIGURE 22. Modified Taylor diagram for *CO* estimation models by using (a) MLR; (b) ANN-MLP; and (c) RF.

of such sensors affected the performance, more specifically, increasing the *rmse*. This drift can be observed in Fig. 23 with normalized raw data of the MQ7 and MG-811 sensors. Interestingly, there is a similar behavior in the signal drift, and the resulting correlation of both of the sensors during the three-months experiment increased to 0.81 from the initial value of 0.09 (see Table 8) during the first 30 days. If the aging model is obtained and introduced in the future estimation models, then the performance may be more consistent after the calibration process ends. This is something that will be considered and evaluated in future research. This is imperative, as the signal drift may increase after the training process.

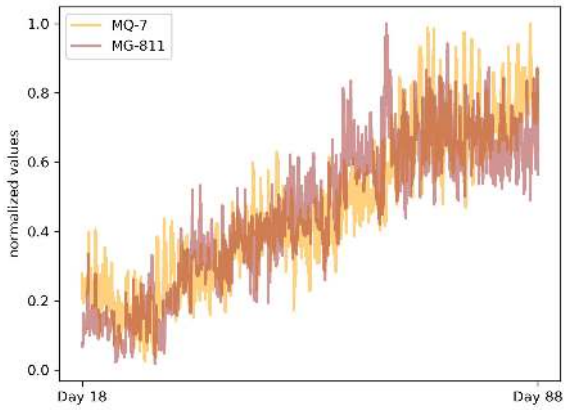

FIGURE 23. Signal drift in CO_X sensors.

The signal drift is notable in the estimations from days 45 to 50, shown in Fig. 24. The boundaries of maximum relative uncertainty are mostly exceeded, specially in concentrations <1.5 *ppm*.

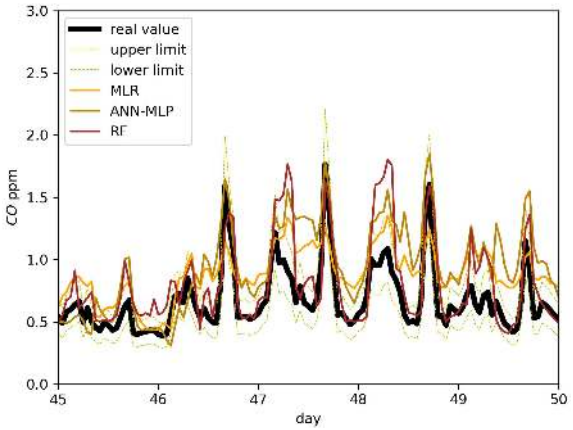

FIGURE 24. Experimental results, *CO* estimation models and relative lower and upper uncertainty boundaries.

VII. CONCLUSION

In this research work, the design, construction and evaluation of a portable station for the measurement of air pollutants has been proposed. The station uses low-cost sensors, off-the-shelve single processing units and data acquisition boards. The two pollutants of interest presented in this investigation are ozone and carbon monoxide. The station was calibrated and evaluated with a certified fixed air monitoring station that was used as the reference terminal, since it complies with the recommendations of the US EPA. Three calibration models are compared: multiple linear regression, artificial neural networks and random forest. To compensate for the deficiencies in the measurements of the low-cost sensors, meteorological variables (humidity and temperature) and a temporal heuristic (timestamp) were included in the model, and a decision rule was implemented to find the optimal sensor combination. The experiment lasted three months, in which different time frames were used for the calibration and evaluation process.

There was an important impact in the quality of information generated by the *CO* estimation models. The performance of metal-oxide sensors seems to be mainly affected by aging, and this parameter is a strong candidate to be evaluated in future research to reduce the estimation error and improve the quality of information. On the other hand, more stable and consistent results were found with the O_3 models, specially with the neural network model. In contrast, the random forest approach does not seem a good candidate to operate with the same accuracy in a time interval different from the training time frame.

Finally, with the low-cost atmospheric pollution station presented in this work, a monitoring network can be created, reducing the costs of implementation and maintenance, as well as having portability and capacity to generate qualitative information of the pollutants of interest in the population. If the information generated from such devices comply with specific standards for air composition measurement, then it could be used by governmental entities during the application of control policies to mitigate air pollution. Other areas of application may include scientific research where air monitoring stations are required to provide accurate measurements to avoid misleading results. Thus, this work has several potential applications aimed to protect the environment, safeguard human health and support scientific research, as previously implemented in [51]–[53].

REFERENCES

[1] World Health Organization. (2016). *Mortality and Burden of Disease From Ambient Air Pollution*. [Online]. Available: https://www.who.int/gho/phe/outdoor_air_pollution/burden/en/

[2] World Health Organization. (2016). *Mortality From Household Air Pollution*. [Online]. Available: https://www.who.int/gho/phe/indoor_air_pollution/burden/en/

[3] World Health Organization. (2016). *Global Urban Ambient Air Pollution Database*. [Online]. Available: https://www.who.int/airpollution/data/cities/en/

[4] S. C. Edwards, W. Jedrychowski, M. Butscher, D. Camann, A. Kieltyka, E. Mroz, E. Flak, Z. Li, S. Wang, V. Rauh, and F. Perera, "Prenatal exposure to airborne polycyclic aromatic hydrocarbons and children's intelligence at 5 years of age in a prospective cohort study in poland," *Environmental Health Perspectives*, vol. 118, no. 9, pp. 1326–1331, Sep. 2010. [Online]. Available: https://ehp.niehs.nih.gov/doi/10.1289/ehp.0901070

[5] C. A. Pope and D. W. Dockery, "Health effects of fine particulate air pollution: Lines that Connect," *J. Air Waste Manage. Assoc.*, vol. 56, no. 6, pp. 709–742, Jun. 2006. [Online]. Available: https://www.tandfonline.com/doi/full/10.1080/10473289.2006.10464485

[6] M. Carugno, D. Consonni, G. Randi, D. Catelan, L. Grisotto, P. A. Bertazzi, A. Biggeri, and M. Baccini, "Air pollution exposure, cause-specific deaths and hospitalizations in a highly polluted Italian region," *Environ. Res.*, vol. 147, pp. 415–424, May 2016. [Online]. Available: https://linkinghub.elsevier.com/retrieve/pii/S0013935116300834

[7] D. M. Stieb, L. Chen, P. Hystad, B. S. Beckerman, M. Jerrett, M. Tjepkema, D. L. Crouse, D. W. Omariba, P. A. Peters, A. van Donkelaar, R. V. Martin, R. T. Burnett, S. Liu, M. Smith-Doiron, and R. M. Dugandzic, "A national study of the association between traffic-related air pollution and adverse pregnancy outcomes in Canada, 1999–2008," *Environ. Res.*, vol. 148, pp. 513–526, Jul. 2016. [Online]. Available: https://linkinghub.elsevier.com/retrieve/pii/S0013935116301487

[8] H. Ritchie and M. Roser. (2019). *Air pollution, Our World in Data*. [Online]. Available: https://ourworldindata.org/air-pollution

[9] G. Hutton. (2011). *Air Pollution: Global Damage Costs of Air Pollution From 1900 to 2050*. Copenhagen Consensus Center, Copenhagen, Denmark. Accessed: Mar. 12, 2020. [Online]. Available: http://www.jstor.org/stable/resrep16318

[10] European Commission TNS Political Social, "Special Eurobarometer 468: Attitudes of European citizens towards the environment," Eur. Comission, Tech. Rep. 2017.6399, Nov. 2017.

[11] *Directive 2008/50/EC*, Eur. Parliament, Brussels, Belgium, May 2008.

[12] Office of Air Quality Planning and Standards, "Technical assistance document for the reporting of daily air quality—The air quality index (AQI)," U.S. Environ. Protection Agency, Research Triangle Park, NC, USA, Tech. Rep. EPA-454/B-18-007, 2018, p. 22.

[13] P. Kumar, L. Morawska, C. Martani, G. Biskos, M. Neophytou, S. Di Sabatino, M. Bell, L. Norford, and R. Britter, "The rise of low-cost sensing for managing air pollution in cities," *Environ. Int.*, vol. 75, pp. 199–205, Feb. 2015. [Online]. Available: https://linkinghub.elsevier.com/retrieve/pii/S0160412014003547

[14] K. Hu, V. Sivaraman, B. G. Luxan, and A. Rahman, "Design and evaluation of a metropolitan air pollution sensing system," *IEEE Sensors J.*, vol. 16, no. 5, pp. 1448–1459, Mar. 2016. [Online]. Available: http://ieeexplore.ieee.org/document/7323791/

[15] L.-J. Chen, Y.-H. Ho, H.-C. Lee, H.-C. Wu, H.-M. Liu, H.-H. Hsieh, Y.-T. Huang, and S.-C.-C. Lung, "An open framework for participatory PM2.5 monitoring in smart cities," *IEEE Access*, vol. 5, pp. 14441–14454, 2017. [Online]. Available: http://ieeexplore.ieee.org/document/7970115/

[16] A. L. Clements, W. G. Griswold, A. Rs, J. E. Johnston, M. M. Herting, J. Thorson, A. Collier-Oxandale, and M. Hannigan, "Low-cost air quality monitoring tools: From research to practice (a workshop Summary)," *Sensors*, vol. 17, no. 11, p. 2478, Oct. 2017. [Online]. Available: http://www.mdpi.com/1424-8220/17/11/2478

[17] B. Maag, Z. Zhou, and L. Thiele, "W-Air: Enabling personal air pollution monitoring on wearables," *Proc. ACM Interact., Mobile, Wearable Ubiquitous Technol.*, vol. 2, no. 1, pp. 1–25, Mar. 2018. [Online]. Available: http://dl.acm.org/citation.cfm?doid=3200905.3191756

[18] M. van den Bossche, N. T. Rose, and S. F. J. De Wekker, "Potential of a low-cost gas sensor for atmospheric methane monitoring," *Sens. Actuators B, Chem.*, vol. 238, pp. 501–509, Jan. 2017. [Online]. Available: https://linkinghub.elsevier.com/retrieve/pii/S0925400516311273

[19] A. Collier-Oxandale, J. G. Casey, R. Piedrahita, J. Ortega, H. Halliday, J. Johnston, and M. P. Hannigan, "Assessing a low-cost methane sensor quantification system for use in complex rural and urban environments," *Atmos. Meas. Techn.*, vol. 11, no. 6, pp. 3569–3594, Jun. 2018. [Online]. Available: https://www.atmos-meas-tech.net/11/3569/2018/

[20] T. Becnel, K. Tingey, J. Whitaker, T. Sayahi, K. Le, P. Goffin, A. Butterfield, K. Kelly, and P.-E. Gaillardon, "A distributed low-cost pollution monitoring platform," *IEEE Internet Things J.*, vol. 6, no. 6, pp. 10738–10748, Dec. 2019. [Online]. Available: https://ieeexplore.ieee.org/document/8836643/

[21] N. Zimmerman, A. A. Presto, S. P. N. Kumar, J. Gu, A. Hauryliuk, E. S. Robinson, A. L. Robinson, and R. Subramanian, "Closing the gap on lower cost air quality monitoring: Machine learning calibration models to improve low-cost sensor performance," *Atmos. Meas. Techn. Discuss.*, pp. 1–36, Aug. 2017. [Online]. Available: https://www.atmos-meas-tech-discuss.net/amt-2017-260/

[22] C. Malings, R. Tanzer, A. Hauryliuk, S. P. N. Kumar, N. Zimmerman, L. B. Kara, A. A. Presto, and R. Subramanian, "Development of a general calibration model and long-term performance evaluation of low-cost sensors for air pollutant gas monitoring," *Atmos. Meas. Techn.*, vol. 12, no. 2, pp. 903–920, Feb. 2019. [Online]. Available: https://www.atmos-meas-tech.net/12/903/2019/

[23] R. Tanzer, C. Malings, A. Hauryliuk, R. Subramanian, and A. A. Presto, "Demonstration of a low-cost multi-pollutant network to quantify intra-urban spatial variations in air pollutant source impacts and to evaluate environmental justice," *Int. J. Environ. Res. Public Health*, vol. 16, no. 14, p. 2523, Jul. 2019. [Online]. Available: https://www.mdpi.com/1660-4601/16/14/2523

[24] N. Castell, F. R. Dauge, P. Schneider, M. Vogt, U. Lerner, B. Fishbain, D. Broday, and A. Bartonova, "Can commercial low-cost sensor platforms contribute to air quality monitoring and exposure estimates?" *Environ. Int.*, vol. 99, pp. 293–302, Feb. 2017. [Online]. Available: https://linkinghub.elsevier.com/retrieve/pii/S0160412016309989

[25] B. Maag, Z. Zhou, and L. Thiele, "A survey on sensor calibration in air pollution monitoring deployments," *IEEE Internet Things J.*, vol. 5, no. 6, pp. 4857–4870, Dec. 2018. [Online]. Available: https://ieeexplore.ieee.org/document/8405565/

[26] L. Spinelle, M. Gerboles, M. G. Villani, M. Aleixandre, and F. Bonavitacola, "Field calibration of a cluster of low-cost available sensors for air quality monitoring. Part A: Ozone and nitrogen dioxide," *Sens. Actuators B, Chem.*, vol. 215, pp. 249–257, Aug. 2015. [Online]. Available: https://linkinghub.elsevier.com/retrieve/pii/S092540051500355X

[27] L. Spinelle, M. Gerboles, M. G. Villani, M. Aleixandre, and F. Bonavitacola, "Field calibration of a cluster of low-cost commercially available sensors for air quality monitoring. Part B: NO, CO and CO_2," *Sens. Actuators B, Chem.*, vol. 238, pp. 706–715, Jan. 2017. [Online]. Available: https://linkinghub.elsevier.com/retrieve/pii/S092540051631070X

[28] Y. Lin, W. Dong, and Y. Chen, "Calibrating low-cost sensors by a two-phase learning approach for urban air quality measurement," *Proc. ACM Interact., Mobile, Wearable Ubiquitous Technol.*, vol. 2, no. 1, pp. 1–18, Mar. 2018. [Online]. Available: http://dl.acm.org/citation.cfm?doid=3200905.3191750

[29] D. H. Hagan, G. Issacman-Vanwertz, J. P. Franklin, L. M. M. Wallace, B. D. Kocar, C. L. Heald, and J. H. Kroll, "Calibration and assessment of electrochemical air quality sensors by co-location with reference-grade instruments," *Atmos. Meas. Techn. Discuss.*, vol. 11, no. 1, pp. 1–40, Aug. 2017. [Online]. Available: https://www.atmos-meas-tech-discuss.net/amt-2017-296/, doi: 10.5194/amt-2017-296.

[30] E. Esposito, S. De Vito, M. Salvato, V. Bright, R. Jones, and O. Popoola, "Dynamic neural network architectures for on field stochastic calibration of indicative low cost air quality sensing systems," *Sens. Actuators B, Chem.*, vol. 231, pp. 701–713, Aug. 2016. [Online]. Available: https://linkinghub.elsevier.com/retrieve/pii/S092540051630332X

[31] S. De Vito, E. Esposito, M. Salvato, O. Popoola, F. Formisano, R. Jones, and G. Di Francia, "Calibrating chemical multisensory devices for real world applications: An in-depth comparison of quantitative machine learning approaches," 2017, *arXiv:1708.09175*. [Online]. Available: http://arxiv.org/abs/1708.09175

[32] N. Zimmerman, A. A. Presto, S. P. N. Kumar, J. Gu, A. Hauryliuk, E. S. Robinson, A. L. Robinson, and R. Subramanian, "A machine learning calibration model using random forests to improve sensor performance for lower-cost air quality monitoring," *Atmos. Meas. Techn.*, vol. 11, no. 1, pp. 291–313, Jan. 2018. [Online]. Available: https://www.atmos-meas-tech.net/11/291/2018/

[33] P. Ferrer-Cid, J. M. Barcelo-Ordinas, J. Garcia-Vidal, A. Ripoll, and M. Viana, "A comparative study of calibration methods for low-cost ozone sensors in IoT platforms," *IEEE Internet Things J.*, vol. 6, no. 6, pp. 9563–9571, Dec. 2019. [Online]. Available: https://ieeexplore.ieee.org/document/8765745/

[34] S. De Vito, E. Esposito, M. Salvato, O. Popoola, F. Formisano, R. Jones, and G. Di Francia, "Calibrating chemical multisensory devices for real world applications: An in-depth comparison of quantitative machine learning approaches," *Sens. Actuators B, Chem.*, vol. 255, pp. 1191–1210, Feb. 2018. [Online]. Available: https://linkinghub.elsevier.com/retrieve/pii/S0925400517313692

[35] K. Alhasa, M. Mohd Nadzir, P. Olalekan, M. Latif, Y. Yusup, M. Iqbal Faruque, F. Ahamad, H. Abd Hamid, K. Aiyub, S. Md Ali, M. Khan, A. A. Samah, I. Yusuff, M. Othman, T. Tengku Hassim, and N. Ezani, "Calibration model of a low-cost air quality sensor using an adaptive neuro-fuzzy inference system," *Sensors*, vol. 18, no. 12, p. 4380, Dec. 2018. [Online]. Available: http://www.mdpi.com/1424-8220/18/12/4380

[36] Z. A. Barakeh, P. Breuil, N. Redon, C. Pijolat, N. Locoge, and J.-P. Viricelle, "Development of a normalized multi-sensors system for low cost on-line atmospheric pollution detection," *Sens. Actuators B, Chem.*, vol. 241, pp. 1235–1243, Mar. 2017. [Online]. Available: https://linkinghub.elsevier.com/retrieve/pii/S092540051631632X

[37] W. Jiao, G. Hagler, R. Williams, R. Sharpe, R. Brown, D. Garver, R. Judge, M. Caudill, J. Rickard, M. Davis, L. Weinstock, S. Zimmer-Dauphinee, and K. Buckley, "Community Air Sensor Network (CAIRSENSE) project: Evaluation of low-cost sensor performance in a suburban environment in the southeastern United States," *Atmos. Meas. Techn.*, vol. 9, no. 11, pp. 5281–5292, Nov. 2016. [Online]. Available: https://www.atmos-meas-tech.net/9/5281/2016/
[38] X. Pang, M. D. Shaw, A. C. Lewis, L. J. Carpenter, and T. Batchellier, "Electrochemical ozone sensors: A miniaturised alternative for ozone measurements in laboratory experiments and air-quality monitoring," *Sens. Actuators B, Chem.*, vol. 240, pp. 829–837, Mar. 2017. [Online]. Available: https://linkinghub.elsevier.com/retrieve/pii/S092540051631437X
[39] C. R. Martin, N. Zeng, A. Karion, R. R. Dickerson, X. Ren, B. N. Turpie, and K. J. Weber, "Evaluation and environmental correction of ambient CO measurements from a low-cost NDIR sensor," *Atmos. Meas. Techn.*, vol. 10, no. 7, pp. 2383–2395, Jul. 2017. [Online]. Available: https://www.atmos-meas-tech.net/10/2383/2017/
[40] X. Pang, M. D. Shaw, S. Gillot, and A. C. Lewis, "The impacts of water vapour and co-pollutants on the performance of electrochemical gas sensors used for air quality monitoring," *Sens. Actuators B, Chem.*, vol. 266, pp. 674–684, Aug. 2018. [Online]. Available: https://linkinghub.elsevier.com/retrieve/pii/S0925400518306427
[41] D. B. Topalović, M. D. Davidović, M. Jovanović, A. Bartonova, Z. Ristovski, and M. Jovašević-Stojanović, "In search of an optimal in-field calibration method of low-cost gas sensors for ambient air pollutants: Comparison of linear, multilinear and artificial neural network approaches," *Atmos. Environ.*, vol. 213, pp. 640–658, Sep. 2019. [Online]. Available: https://linkinghub.elsevier.com/retrieve/pii/S1352231019304194
[42] B. Tian, K. M. Hou, X. Diao, H. Shi, H. Zhou, and W. Wang, "Environment-adaptive calibration system for outdoor low-cost electrochemical gas sensors," *IEEE Access*, vol. 7, pp. 62592–62605, 2019. [Online]. Available: https://ieeexplore.ieee.org/document/8715507/
[43] S. Moltchanov, "On the feasibility of measuring urban air pollution by wireless distributed sensor networks," *Sci. Total Environ.*, vol. 502, pp. 537–547, Jan. 2015.
[44] C. Lin, "Evaluation and calibration of Aeroqual series 500 portable gas sensors for accurate measurement of ambient ozone and nitrogen dioxide," *Atmos. Environ.*, vol. 100, pp. 111–116, Jan. 2015.
[45] C. Borrego, A. M. Costa, J. Ginja, M. Amorim, M. Coutinho, K. Karatzas, T. Sioumis, N. Katsifarakis, K. Konstantinidis, S. De Vito, E. Esposito, P. Smith, N. André, P. Gérard, L. A. Francis, N. Castell, P. Schneider, M. Viana, M. C. Minguillón, W. Reimringeri, "Assessment of air quality microsensors versus reference methods: The EuNetAir joint exercise," *Atmos. Environ.*, vol. 147, pp. 246–263, Dec. 2016. [Online]. Available: https://linkinghub.elsevier.com/retrieve/pii/S1352231016307610
[46] P. R. Espinoza, Claudia. (2017). *SpanishInforme de Calidad del Aire–Cuenca 2017*. [Online]. Available: https://www.researchgate.net/publication/328615569_Informe_de_Calidad_Aire_Cuenca_2017
[47] *Technical Manual—Model 300e Family CO Analyzers*, Teledyne, Teledyne Adv. Pollut. Instrumentation, San Diego, CA, USA, Jan. 2009.
[48] *Technical Manual—Model 400e Photometric Ozone Analyzer*, Teledyne, Teledyne Adv. Pollution Instrum., San Diego, CA, USA, May 2011.
[49] F. Pedregosa, G. Varoquaux, A. Gramfort, V. Michel, B. Thirion, O. Grisel, M. Blondel, P. Prettenhofer, R. Weiss, V. Dubourg, J. Vanderplas, A. Passos, D. Cournapeau, M. Brucher, M. Perrot, and E. Duchesnay, "Scikit-learn: Machine learning in Python," *J. Mach. Learn. Res.*, vol. 12, pp. 2825–2830, 2011.
[50] A. Paszke, S. Gross, S. Chintala, G. Chanan, E. Yang, Z. DeVito, Z. Lin, A. Desmaison, L. Antiga, and A. Lerer, "Automatic differentiation in PyTorch," in *Proc. NeurIPS Autodiff Workshop*, 2017, pp. 1–4.
[51] K. R. Mallires, D. Wang, V. V. Tipparaju, and N. Tao, "Developing a low-cost wearable personal exposure monitor for studying respiratory diseases using metal–oxide sensors," *IEEE Sensors J.*, vol. 19, no. 18, pp. 8252–8261, Sep. 2019. [Online]. Available: https://ieeexplore.ieee.org/document/8717689/
[52] B. Zhang, T. Xi, X. Gong, and W. Wang, "Mutual information maximization-based collaborative data collection with calibration constraint," *IEEE Access*, vol. 7, pp. 21188–21200, 2019. [Online]. Available: https://ieeexplore.ieee.org/document/8626122/
[53] L. Lombardo, M. Parvis, E. Angelini, and S. Grassini, "An optical sampling system for distributed atmospheric particulate matter," *IEEE Trans. Instrum. Meas.*, vol. 68, no. 7, pp. 2396–2403, Jul. 2019. [Online]. Available: https://ieeexplore.ieee.org/document/8627977/

GALO D. ASTUDILLO was born in Cuenca, Ecuador, in 1994. He received the Electronics and Telecommunications Engineering degree from the Universidad de Cuenca, Ecuador, in 2018.

From 2017 to 2018, he was a Research Assistant with the Electric, Electronics and Telecommunications Department, Universidad de Cuenca. Since 2019, he has been a Research Assistant with the Mechatronics Department, Tecnológico de Monterrey, Monterrey. His research interests include embedded systems, machine learning, mechatronics, and image processing.

LUIS E. GARZA-CASTAÑON was born in Monclova, Coahuila, Mexico, in 1963. He received the Engineering degree in electronic systems, the M.Sc. degree in control engineering, and the Ph.D. degree in artificial intelligence from Tecnológico de Monterrey, Monterrey, Mexico, in 1986, 1988, and 2001, respectively.

From 1999 to 2003, he was a Lecturer with the Physics Department, Tecnologico de Monterrey. Since 2004, he has been an Associate Professor with the Mechatronics Department, Tecnológico de Monterrey. He is the author of more than 100 articles. His research interests include machine learning, fault detection, diagnosis and control, image processing, and advanced control applications.

LUIS I. MINCHALA AVILA (Senior Member, IEEE) received the B.S.E.E. degree from the Salesian Polytechnic University, Cuenca, Ecuador, in 2006, and the M.Sc. and Ph.D. degrees from the Instituto Tecnológico y de Estudios Superiores de Monterrey, Monterrey, Mexico, in 2011 and 2014, respectively. From summer 2012 to summer 2013, he was a Visiting Scholar with Concordia University, Montreal, QC, Canada. From 2017 to 2018, he was a Postdoctoral Fellow with the Climate Change Research Group, Tecnológico de Monterrey. He is currently a full-time Researcher with the School of Engineering and Sciences, Tecnológico de Monterrey, Guadalajara, Mexico. He has authored and coauthored over 40 indexed publications, including journal articles, conference proceedings, book chapters, and a book.